

# **Risk assessment of dangerous products release and dispersion: a comparison between CFD and integral models**

A. Fiorucci<sup>1</sup>, M. Pontiggia<sup>1</sup>, M. Derudi<sup>1</sup>, M. Alba<sup>2</sup>, M. Scaioni<sup>2</sup>, R. Pendino<sup>3</sup>,  
G. Uguccioni<sup>3</sup>, R. Rota<sup>1</sup>

<sup>1</sup> Dip. di Chimica, Materiali e Ingegneria Chimica “G. Natta”, Politecnico di Milano, via Mancinelli 7, 20131-Milano, Italy

<sup>2</sup> Dip. Di Ing. Idraulica, Ambientale, delle Infrastrutture Viarie e del Rilevamento, Politecnico di Milano, Corso Promessi Sposi 29, 23900-Lecco, Italy

<sup>3</sup> D'Appolonia S.p.A. - via Martiri di Cefalonia 2, 20097-San Donato Milanese (MI) - Italy

The main aim of this study is the comparison between results obtained by integral models and computational fluid dynamics codes in order to verify the more suitable approach in gas releases prediction. Experimental data were used to validate the models used by CFD codes. A complete set of boundary conditions (wind, temperature, turbulence profiles) was also developed to consider the influence of atmospheric turbulence, actually only for the neutral stratification (i.e. stability class D).

The CFD turbulence model (k-epsilon) was slightly modified in order to achieve the consistency between the Monin-Obukhov profiles and the transport equation of the turbulent dissipation.

Results showed a good agreement between the previsions of the two approaches for open field releases. On the contrary, geometrically complex scenarios make integral models inaccurate and require CFD simulations in order to obtain reasonable data.

## **1. Introduction**

In safety studies concerning consequences analysis of gas releases, integral methods are widely used in order to obtain previsions of the dimensions of the area involved by the dispersion (Bernatik and Libisova, 2004). They are easy and low time-consuming tools, but they are liable to some deficiencies (one-dimensional modelling) and obey to certain assumptions. On the other hand, powerful computational tools based on fluid dynamics methods have recently been developed (Computational Fluid Dynamics, CFD) allowing for an integrated approach on complex scenarios and/or physicochemical phenomena. CFD codes perform three-dimensional computations of fluid properties variation, turbulence modelling, chemical reactions, in addition to accurately represent the geometry of the flow field. However, this level of details could be time-consuming.

The prediction of an accidental gas release, in term of both people and area involved by a toxic or flammable cloud dispersion, is of paramount importance for the definition of safety plans and actions to be undertaken to avoid and/or mitigate the consequences of such an accident; for this reason, the purpose of this work was to point out that CFD

approach cannot be given up when geometrically complex scenarios are considered. Two commercial suites, a general purpose commercial CFD code and the PHAST model (integral model) were used for the comparison. For CFD simulations, accordingly to literature (Luketa-Hanlin et al., 2007), standard k-ε model for turbulence was used.

$$\frac{\partial}{\partial t}(\rho k) + \frac{\partial}{\partial x_i}(\rho k u_i) = \frac{\partial}{\partial x_j} \left[ \left( \mu + \frac{\mu_T}{\sigma_k} \right) \frac{\partial k}{\partial x_j} \right] + G_k + G_b - \rho \varepsilon - Y_M \quad (1)$$

$$\frac{\partial}{\partial t}(\rho \varepsilon) + \frac{\partial}{\partial x_i}(\rho \varepsilon u_i) = \frac{\partial}{\partial x_j} \left[ \left( \mu + \frac{\mu_T}{\sigma_\varepsilon} \right) \frac{\partial \varepsilon}{\partial x_j} \right] + C_{1\varepsilon} \frac{\varepsilon}{k} (G_k + C_{3\varepsilon} G_b) - C_{2\varepsilon} \rho \frac{\varepsilon^2}{k} + S_\varepsilon \quad (2)$$

Where  $\rho$  is gas density,  $u_i$  the  $i$ -th velocity component,  $\mu$  air viscosity,  $\mu_T$  turbulent air viscosity,  $G_k$ ,  $G_b$ ,  $Y_M$  are k production terms due to the shear stress, buoyancy and pressure gradient, respectively.  $\sigma_k$ ,  $\sigma_\varepsilon$ ,  $C_{1\varepsilon}$ ,  $C_{2\varepsilon}$ ,  $C_{3\varepsilon}$  are k-ε model constants ( $\sigma_k=1$ ,  $\sigma_\varepsilon=1.3$ ,  $C_{1\varepsilon}=1.44$ ,  $C_{2\varepsilon}=1.92$ ,  $C_{3\varepsilon}=1.0$ ).

## 2. Open field releases

First of all, to ensure the validity of CFD codes predictions, an experimental release was simulated and the predictions of this simulation compared with experimental data and PHAST results. Prairie Grass experimental set was selected (Holt & Witlox, 2000); a small quantity of sulphur dioxide was released at or near ground level over a flat terrain. Experiments were carried out during both daylight and night hours with the aim to study a wide range of atmospheric stability conditions. Concentrations of SO<sub>2</sub> were measured from an array of sensors located on arcs at downwind distances of 50, 100, 200, 400 and 800 [m]. It is worth to be noticed that this experimental dataset was used for the tuning of PHAST parameters; so a good agreement between its predictions and field measurements was expected.

By now only neutral stratification was investigated because of the simpler boundary conditions it requires. So, test 17 (Pasquill class D) of Prairie Grass experiments was reproduced.

### 2.1 Boundary condition

Preliminary simulations were conducted choosing constant profiles of wind speed, air temperature, turbulent kinetic energy  $k$  and turbulent dissipation rate  $\varepsilon$  as boundary conditions for the wind inlet surface. It was observed that, even in open field, the imposed profiles change drastically, leading to two opposite effects: a progressive increase of turbulence intensity near the ground due to the terrain roughness, and to a quick disappearance of turbulent intensity away from ground level due to the lack of shear stress in the flat-profile of the air flow.

### 2.2 Atmospheric profile

In order to describe the atmospheric flow over uniform flat terrain, expressions based on the Monin-Obukhov similarity theory from Panofsky and Dutton (1984) have been

considered. The turbulent viscosity  $\mu_T$  is expressed as a function of the mixing length; for neutral stratification it results:

$$\mu_T(z) = \rho K u_* z \quad (3)$$

$$u_* = \sqrt{\frac{\tau_w}{\rho}} \quad (4)$$

where  $K$  is the von Karman constant ( $K=0.42$ ),  $z$  the vertical coordinate ( $z=0$  at ground),  $u_*$  the turbulent friction velocity,  $\tau_w$  the surface shear stress and  $g$  the gravitational acceleration module.

Assuming the shear stress and heat flux to be constant over the lower part of the atmospheric boundary layer, modified logarithmic velocity and temperature profiles for neutral stratification can be computed:

$$u(z) = \frac{u_*}{K} \ln\left(\frac{z}{z_0}\right) \quad (5)$$

$$T(z) - T_w = -\frac{g}{c_p}(z - z_0) \quad (6)$$

where  $z_0$  corresponds to the roughness length of the site,  $T_w$  is the ground temperature and  $c_p$  the air heat capacity at constant pressure. In CFD simulations the approximation of incompressible gas was taken for air; therefore it is impossible to balance the adiabatic profile of temperature (6) varying the pressure along  $z$ -direction. As a consequence, a reduced temperature, which is constant for neutral stratification, was considered:

$$\theta = T(z) + \frac{g}{c_p}(z - z_0) = T_w \quad (7)$$

Rearranging the transport equations of turbulent kinetic  $k$  energy (1) with equations (3) and (5) for steady case, over a flat terrain (null gradients along  $x$  and  $y$  directions) one can find:

$$\varepsilon(z) = \frac{u_*^3}{Kz} \quad (8)$$

$$k = \frac{u_*^2}{\sqrt{C_\mu}} \quad (9)$$

where  $C_\mu$  is a  $k$ - $\varepsilon$  model constant ( $C_\mu=0.09$ ). In order to ensure the consistency between these profiles and turbulent dissipation rate equation, Alinot & Masson (2005) suggested to alter the  $k$ - $\varepsilon$  model constants. This solution, however, while grants good

performances for the evaluation of atmospheric profiles over flat terrains, has not been tested for the prediction of turbulence due to obstacles. For this reason, it was preferred to add a z-dependent term ( $S_\varepsilon$ ) to the  $\varepsilon$  equation (2):

$$S_\varepsilon(z) = \frac{\rho u_*^4}{z^2} \left[ \frac{(C_{2\varepsilon} - C_{1\varepsilon}) \sqrt{C_\mu}}{K^2} - \frac{1}{\sigma_\varepsilon} \right] - \mu \frac{u_*^3}{2Kz^3} \quad (11)$$

Figure 1 shows a comparison of the profiles of turbulent kinetic energy  $k$  at the inlet and at the outlet of a 300 [m] long computational domain. It is possible to notice that the difference between the mean-values of  $k$  is lower than 4%.

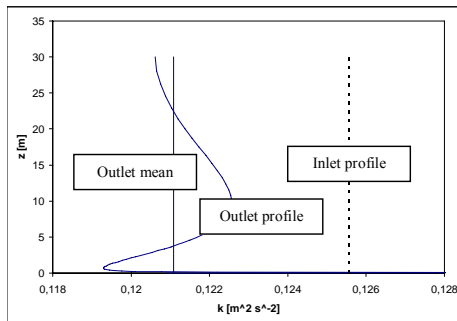


Figure 1 – Turbulent kinetic energy profiles at the domain boundaries

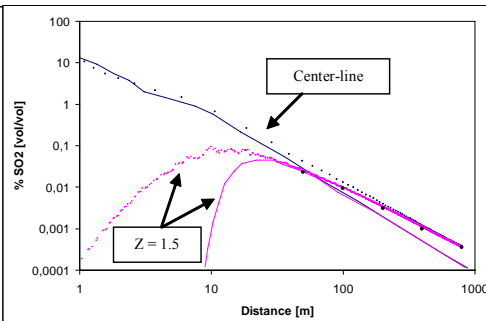


Figure 2 – Comparison between CFD (dotted lines) and integral methods (solid lines):  $SO_2$  open-field dispersion

### 2.3 Results

Figure 2 shows a comparison between CFD and integral methods results for an open field dispersion (Prairie Grass, test 17). Dotted lines represent CFD predictions, while solid lines PHAST simulations; two concentration profiles are reported: along the center-line and at a fixed elevation ( $z = 1.5$  [m]), respectively. It was found a good agreement between PHAST and CFD center-line profiles, especially in the near-field ( $x < 10$  [m]). On the other hand, in this range, profiles at fixed elevation substantially disagree. This is because PHAST, due to its assumptions, is unable to correctly predict the behaviour of the gas dispersion close to the source, while it is expected to well reproduce field data far from the emitting source. Nevertheless, CFD results show an agreement with experimental data as good as PHAST, even if this set has been used for PHAST-parameters tuning.

### 3. Geometrically complex scenarios

A second attempt was made to have a comparison between simulations obtained by CFD and integral methods in presence of obstacles. Two different scenarios were studied: a LNG dispersion within an industrial site, and a pool evaporation of ammonia in an urban area.

### 3.1 LNG Regassifier

A regassifier-like geometry was proposed (Figure 3a), in order to study a Liquefied Natural Gas dispersion case; results were checked in terms of maximum distance for half lower flammability limit (LFL/2) and upper flammability limit (UFL) reached by the cloud.

The dispersion modelling software (PHAST) was used to model a leak in a LNG pipeline, a pool formation and its subsequent evaporation; the total mass discharged was the amount between two shut-down valves. From the PHAST outputs, maximum distances for LFL/2 and UFL were collected, together with the profile of the vaporized mass flow rate of CH<sub>4</sub> and the averaged pool radius to be used as an input for CFD simulations.

The use of the same input conditions for the source description is supposed to ensure a significant comparison between the investigated models.

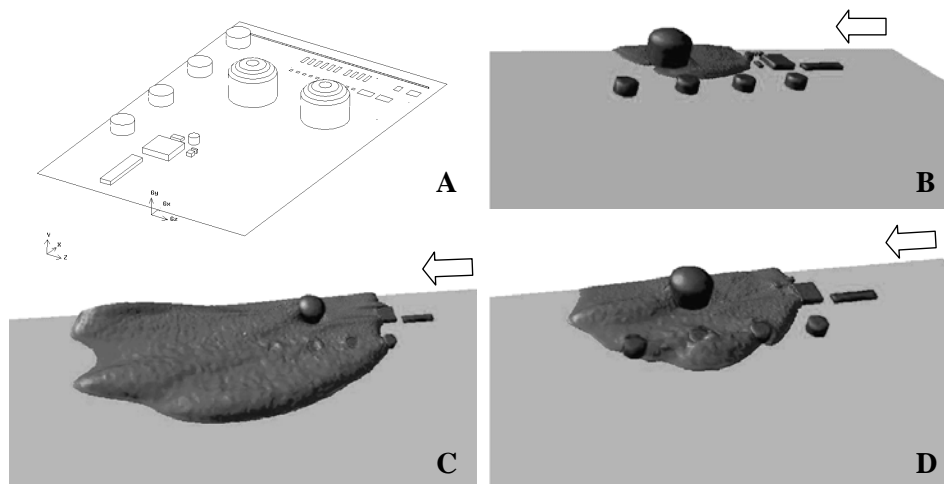


Figure 3 – Hypothetical Regassifier geometry (A), and LFL/2 limits at three different times: cloud passed the tank (B), exceeded the industrial site (C), reached the maximum distance (D); wind speed 5 [m/s], white arrows represent wind direction

Three different geometrical configurations were studied via CFD; the first analysis concerned an open field configuration. This constitutes the basic case study for a comparison with PHAST results. Moreover, since a CFD simulation of a full detailed plant geometry requires an expensive computational effort, resulting in a too time-consuming approach, the open field case study was practically used to define the lower dimensions of the obstacles (namely, plant equipments) that can actually influence the gas cloud dispersion. In fact, a typical regassifier plant can be partitioned in few zones: an uploading platform where ships dock, a pipeline that in some cases is buried, tanks for LNG storage (usually two or more), vaporizers and pumps; all of these equipments have extremely different dimensions and an open field simulation, providing the mean cloud dimensions, can help to simplify the geometry.

The equations used to model the problem were thermal and i-species balances, continuity, turbulence and motion equations.

*Table 1 – Comparison of PHAST and CFD results; wind speed 5 [m/s]. Distances are expressed in [m]*

Case	# cells	Max Dist LFL/2	Max Height LFL/2	Max Dist UFL	Max Height UFL
PHAST	-	1639	15.5	289	5.5
Open field	1000 k	1392	13.6	270	5.8
No wall	1400 k	960	22.0	263	4.0
Wall	1500 k	587	20.0	235	4.5

Main results are summarized in Table 1; it is possible to notice that, for the open field case, results obtained by CFD simulations show a good match, both in terms of LFL/2 and UFL, with PHAST predictions; even though it is possible to notice that CFD predictions only apparently underestimates the LFL/2 distance, because this is coherent with the studies of Pitblado et al. (2006), which underline that PHAST usually over predicts the experimental data concerning LNG clouds. A first important result of this analysis is that it allowed to neglect all the small size elements inside the domain (mainly pipelines, pumps and vaporizers) and their effect on air/gas mixing; this is possible because of the different dimensions of the cloud versus the objects, leading just to a small over prediction of the maximum distances. Therefore a geometry was proposed (Figure 3a) where all objects have dimensions comparable with those of the dispersion; besides, two different geometries were simulated, without and with a 5 [m] height wall, downwind respect to the tanks. For the first case, the maximum distances for LFL/2 decrease significantly, because of the effect of the turbulence mainly due to the tanks. Much less effect is on the UFL distances results: this happens because the objects also tend to concentrate the fluid near the vaporization zone, since a high density fluid behaves similarly to a liquid. Another interesting feature concerns the rise in height with complex geometries, due to the perturbed wind profile near the obstacles. For the wall case, another strong reduction of the maximum distance for LFL/2 can be noticed, due to the presence of a wall at the end of the industrial site that both increases the air entrainment within the cloud and deviates the cloud at the beginning of the dispersion. Much less effect is on the UFL distances, since are smaller than the wall - source distance.

### 3.2 Urban scenario

The geometry of an urban area was also considered. The Lecco (Italy) municipality was chosen because a 3-D topographic map at large scale (1:1k) was available. The geometric features, originally stored in SHP ESRI® format and then transformed in IGES format, were directly imported in the mesh-building software. Here the 3-D urban geometry were cleaned up in order to remove small details which have little influence in gas dispersion related to the cell refinement they require; the minimum detail level considered was about 20 [cm]. The domain dimensions were 300 [m] length, 250 [m] depth, 100 [m] height, for about 1500k cells. Figure 4 reports an aerial orthophoto and a 3-D geometry of the considered area in Lecco.

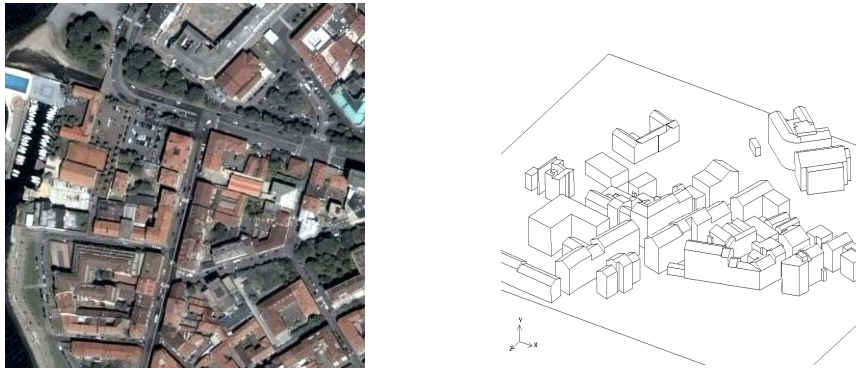


Figure 4 – Orthophoto and original 3-D model of the considered area in Lecco

An evaporation of ammonia from a pool of ammonia-water solution was considered as accidental scenario; as in the former case, PHAST was used to evaluate the pool radius and temperature; then, averaged values were calculated in order to simplify the source term. Dispersion from a steady-state source was modelled with PHAST and simulated with CFD both in open field and in the urban scenario using diffusion from a surface with a constant ammonia fraction. Open field simulation was used to ensure agreement between PHAST predictions of ammonia flow rate and rate of gas diffusion in CFD simulations.

Preliminary steady-state simulations were performed, since they require less computational efforts; the effect of two different wind directions, both with a wind magnitude of 5 [m/s] were investigated. As shown in Figure 5 PHAST obviously cannot distinguish among the two situations, while the CFD code can consider the influence of different obstacles configurations. With the first wind direction (Figure 5a) the cloud is channelled in an urban canyon, roughly directed as the wind itself; as a result, CFD predictions resembles PHAST outcomes, at least far from the pool location. An angled wind direction (Figure 5b) lead, instead, to an extremely tortuous path for the ammonia cloud; this feature makes PHAST predictions clearly inaccurate.

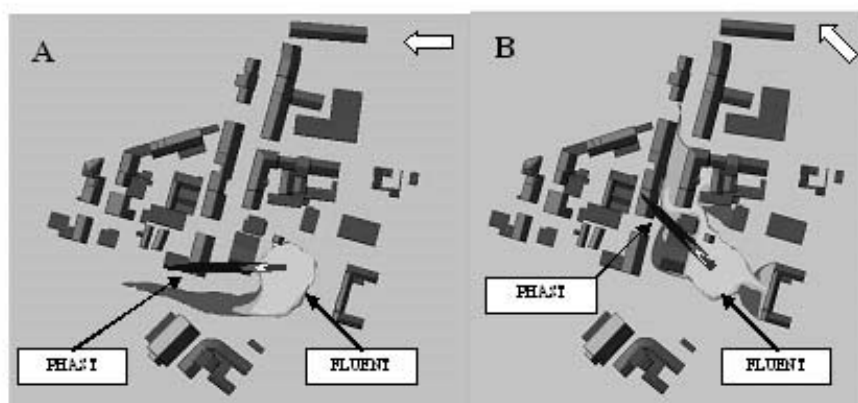


Figure 5 – Ammonia isoconcentrations (1000, 3000, 5000 ppm); white arrows represent wind direction

The second simulation (angled wind direction) was repeated in transient-state in order to evaluate probit values. Results are shown in figure 6. As previously mentioned, CFD provides more realistic outcomes for both width and cloud shape in more complex environments. Figure 6 shows, in particular, as stagnating zones still keep a high dose of toxic gas, raising heavily the probit in zone quite far from the risk maximum distance computed by PHAST.

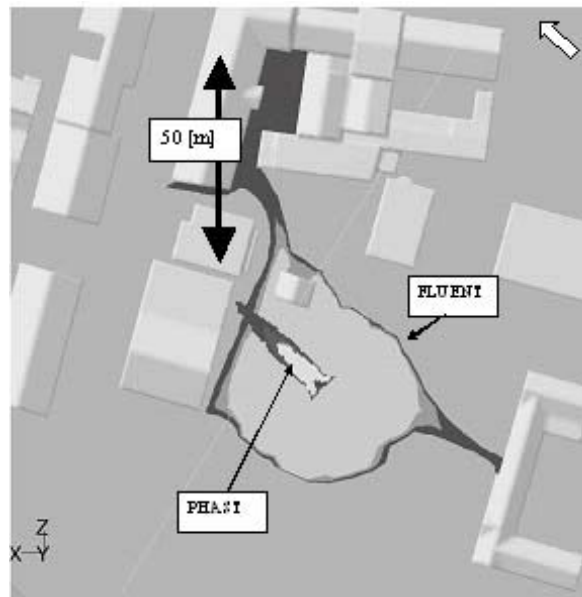


Figure 6 – Iso-Probit zones (2, 3, 4); white arrow represents the wind direction

## 5. References

- Alinot, C., C. Masson, 2005, *J. Solar Energy Engineering* 127, 438
- Bernatik, A., M. Libisova, 2004, *J. Loss Prev. Proc. Ind.* 17, 271
- Luketa-Hanlin, A., R.P. Koopman, D.L. Ermak, 2007, *J. Haz. Mat.* 140, 504
- Holt, A., H.W.M. Witlox, March 1999, *Validation of the unified dispersion model*, Technical reference manual, v. 6.0. DNV, London.
- Panofsky, H., J. Dutton, 1984, *Atmospheric turbulence*, Wiley. New York
- Pitblado R., J. Baikl and V. Raghunathan, 2006, *J. Haz. Mat.* 130, 148

## Acknowledgements

The authors express their thanks to DPC/CONPRICI for the financial support.